

ARTICLE

ON and OFF starburst amacrine cells are controlled by distinct cholinergic pathways

 Mie Gangi¹ , Takuma Maruyama¹ , Toshiyuki Ishii¹ , and Makoto Kaneda¹ 

Cholinergic signaling in the retina is mediated by acetylcholine (ACh) released from starburst amacrine cells (SACs), which are key neurons for motion detection. SACs comprise ON and OFF subtypes, which morphologically show mirror symmetry to each other. Although many physiological studies on SACs have targeted ON cells only, the synaptic computation of ON and OFF SACs is assumed to be similar. Recent studies demonstrated that gene expression patterns and receptor types differed between ON and OFF SACs, suggesting differences in their functions. Here, we compared cholinergic signaling pathways between ON and OFF SACs in the mouse retina using the patch clamp technique. The application of ACh increased GABAergic feedback, observed as postsynaptic currents to SACs, in both ON and OFF SACs; however, the mode of GABAergic feedback differed. Nicotinic receptors mediated GABAergic feedback in both ON and OFF SACs, while muscarinic receptors mediated GABAergic feedback in ON SACs only in adults. Neither tetrodotoxin, which blocked action potentials, nor LY354740, which blocked neurotransmitter release from SACs, eliminated ACh-induced GABAergic feedback in SACs. These results suggest that ACh-induced GABAergic feedback in ON and OFF SACs is regulated by different feedback mechanisms in adults and mediated by non-spiking amacrine cells other than SACs.

Introduction

Visual signals in the retina are processed in parallel between the ON and OFF pathways. Parallel processing starts at bipolar cells. The signals of ON bipolar cells are passed to ON retinal ganglion cells (RGCs) in sublamina b of the inner plexiform layer (IPL), while those of OFF bipolar cells are passed to OFF RGCs in sublamina a of the IPL (Famiglietti and Kolb, 1976; Famiglietti et al., 1977; Nelson et al., 1978). These ON and OFF signals are further processed individually by synaptic inputs from amacrine cells at each sublamina of the IPL. To achieve parallel processing in the IPL, starburst amacrine cells (SACs), important cholinergic neurons in the retina (Taylor and Smith, 2012), have developed two subpopulations: ON and OFF SACs, with similar morphological characteristics, except for their histological localization in the retina (Fig. 1 A). The mirror symmetry of their morphologies strongly suggests similarities in their physiological properties. However, we previously demonstrated that signal processing mechanisms between ON and OFF SACs were not mirror images (P2X₂ receptors: Kaneda et al., 2004, 2008; glycine receptors: Ishii and Kaneda, 2014; and choline transporter: Ishii et al., 2017). These findings were supported by another study showing that ON and

OFF SACs differed at the gene expression level (Peng et al., 2020).

Since SACs play a key role in the formation of direction selectivity, signal processing mechanisms at synapses between SACs and DSGCs have been an attractive target as a model circuit in neural computation (He and Masland, 1997; Yoshida et al., 2001; Amthor et al., 2002; Fried et al., 2002; Lee et al., 2010; Briggman et al., 2011). SACs function as the only cholinergic neurons in the retina (Masland and Mills, 1979; Famiglietti, 1983; Masland et al., 1984; Tauchi and Masland, 1984; Schmidt et al., 1985; Voigt, 1986) and simultaneously work as GABAergic neurons. Asymmetric GABAergic inputs from SACs to direction-selective RGCs are currently recognized as the neural basis for direction selectivity (Fried et al., 2002; Lee et al., 2010; Briggman et al., 2011; Pei et al., 2015). On the other hand, the role of acetylcholine (ACh) remains unclear. Previous studies reported that ACh regulated the activity of RGCs by activating muscarinic (Straschill and Perwein, 1973; Schmidt et al., 1987) and nicotinic receptors (Ikeda and Sheardown, 1982; Schmidt et al., 1987), whereas electrophysiological recordings from RGCs revealed the presence of nicotinic receptors, but not muscarinic receptors

¹Department of Physiology, Nippon Medical School, Tokyo, Japan.

Correspondence to Mie Gangi: m-gangi@nms.ac.jp

T. Maruyama's current affiliation is Division of Neurophysiology, Department of Physiology, School of Medicine, Tokyo Women's Medical University, Tokyo, Japan.

© 2024 Gangi et al. This article is distributed under the terms of an Attribution-Noncommercial-Share Alike-No Mirror Sites license for the first six months after the publication date (see <http://www.upress.org/terms/>). After six months it is available under a Creative Commons License (Attribution-Noncommercial-Share Alike 4.0 International license, as described at <https://creativecommons.org/licenses/by-nc-sa/4.0/>).

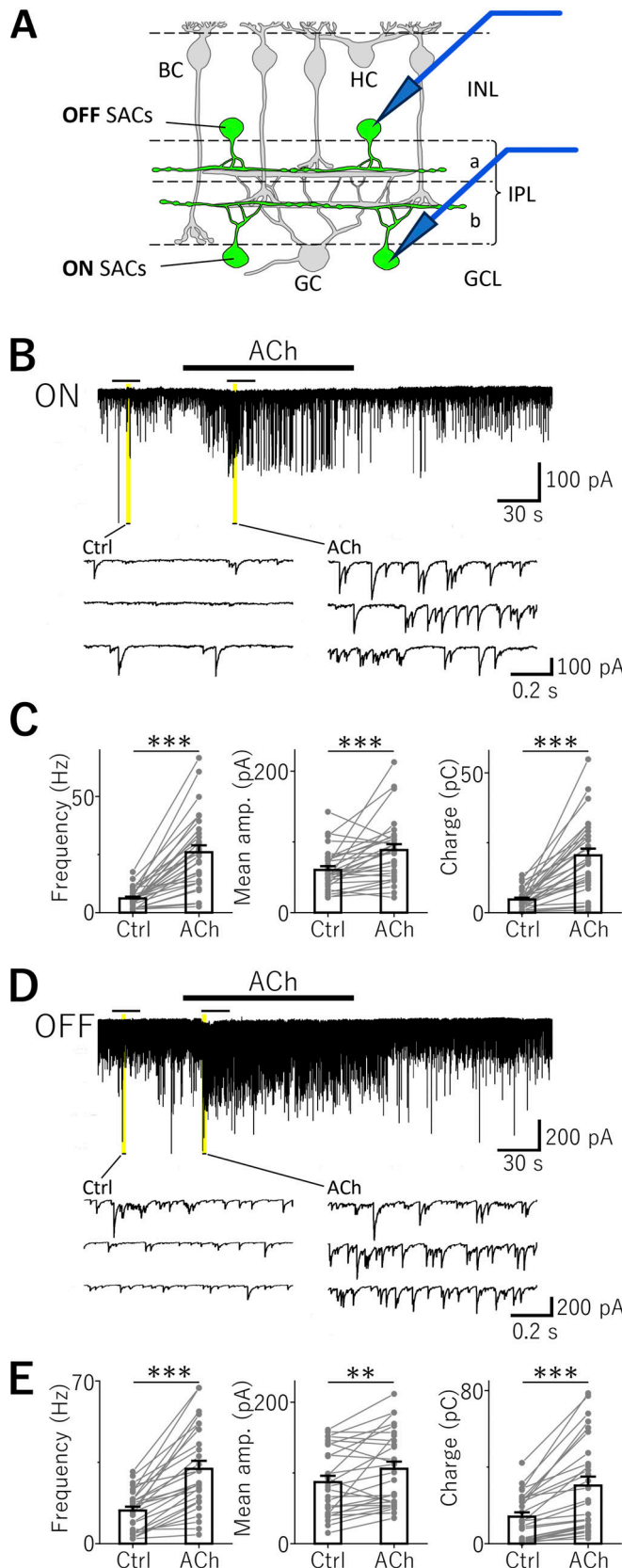


Figure 1. Acetylcholine increased postsynaptic currents (PSCs) in starburst amacrine cells (SACs). (A) Schematic diagram showing a cross-section of the retina. ON or OFF SACs labeled by GFP (green) were targeted. ON and OFF SACs were identified by the location of their soma. BC, bipolar cell; HC, horizontal cell; GC, ganglion cell; INL, inner nuclear layer; IPL, inner plexiform layer; a, sublamina a; b, sublamina b; GCL, ganglion cell layer. (B and D) Effects of ACh in an ON SAC (B) and OFF SAC (D). The thick black bar above the trace shows the timing of the ACh application. Thin black bars show the analysis time windows (20 s) of PSCs. These analysis time windows were set before (Ctrl) and during (ACh) the application of ACh. Bottom: Magnified display of the current trace before (Ctrl: left) and during (ACh: right) the application of ACh (highlighted in yellow). (C and E) Summary of ACh effects on the frequency (left), mean amplitude (middle), and averaged charge transfer (right) of PSCs in ON SACs (C: frequency, $P = 2.09 \times 10^{-8}$; mean amp., $P = 0.000656$; charge, $P = 5.88 \times 10^{-8}$; $n = 29$ cells from 23 mice) and OFF SACs (E: frequency, $P = 8.27 \times 10^{-8}$; mean amp., $P = 0.00481$; charge, $P = 4.12 \times 10^{-6}$; $n = 27$ cells from 21 mice). Data represent means \pm SEM. A paired t -test was used. ** $P < 0.01$, *** $P < 0.001$.

(Lipton et al., 1987; Yazejian and Fain, 1993; Kaneda et al., 1995). Moreover, the contribution of cholinergic inputs to direction selectivity remains controversial. Some studies reported no or a weak impact of ACh on direction selectivity (Ariel and Daw, 1982; Cohen and Miller, 1995; He and Masland, 1997; Kittila and Massey, 1997; Chiao and Masland, 2002; Reed et al., 2002; Park et al., 2014), whereas others demonstrated the importance of cholinergic inputs for direction selectivity (Grzywacz et al., 1998a, 1998b; Reed et al., 2004; Sethuramanujam et al., 2016; Brombas et al., 2017). While the physiological contribution of cholinergic inputs to the formation of direction selectivity has been examined in detail in direction-selective RGCs, limited information is currently available at the amacrine cell level (Myhr and McReynolds, 1996; Neal et al., 2001; Elgueta et al., 2015). Furthermore, the effects of ACh on SACs remain unclear even though reciprocal synapses have been detected between SACs (Zheng et al., 2004). Therefore, a more detailed understanding of the functional role of ACh in retinal circuits is needed.

In the present study, we investigated the physiological properties of cholinergic circuits in ON and OFF SACs to elucidate the neural basis for cholinergic circuits in direction selectivity. The results obtained revealed that ACh increased GABAergic inputs onto ON and OFF SACs. We also showed that these inputs were regulated by muscarinic and nicotinic receptors in ON SACs, but only by nicotinic receptors in OFF SACs. In the previous model of direction selectivity, ACh was considered to function at the level of direction-selective RGCs. The presence of asymmetric neural circuits for ACh-mediated GABAergic regulation between ON and OFF SACs indicates that a more detailed analysis of cholinergic inputs at multiple synapses is needed to elucidate the mechanisms underlying the formation of direction selectivity.

Materials and methods

Animals

The research protocol was approved by the Animal Experiments Ethical Review Committee of Nippon Medical School. The IG-8 transgenic mouse line, which expresses GFP signals in SACs in the retina (Watanabe et al., 1998; Yoshida et al., 2001), of both sexes was used in the present study. P7–8 and adult mice (≥ 4 -wk-old) were used in developmental experiments, and 2–3-wk-old mice in the other experiments.

horizontal cell; GC, ganglion cell; INL, inner nuclear layer; IPL, inner plexiform layer; a, sublamina a; b, sublamina b; GCL, ganglion cell layer. (B and D) Effects of ACh in an ON SAC (B) and OFF SAC (D). The thick black bar above the trace shows the timing of the ACh application. Thin black bars show the analysis time windows (20 s) of PSCs. These analysis time windows were set before (Ctrl) and during (ACh) the application of ACh. Bottom: Magnified display of the current trace before (Ctrl: left) and during (ACh: right) the application of ACh (highlighted in yellow). (C and E) Summary of ACh effects on the frequency (left), mean amplitude (middle), and averaged charge transfer (right) of PSCs in ON SACs (C: frequency, $P = 2.09 \times 10^{-8}$; mean amp., $P = 0.000656$; charge, $P = 5.88 \times 10^{-8}$; $n = 29$ cells from 23 mice) and OFF SACs (E: frequency, $P = 8.27 \times 10^{-8}$; mean amp., $P = 0.00481$; charge, $P = 4.12 \times 10^{-6}$; $n = 27$ cells from 21 mice). Data represent means \pm SEM. A paired t -test was used. ** $P < 0.01$, *** $P < 0.001$.

Preparations

We followed the methods described in our previous studies (Ishii and Kaneda, 2014; Ishii et al., 2017). In brief, animals were euthanized by cervical dislocation and both eyes were enucleated. Eyes were hemisected and retinae were isolated from sclera in Ringer's solution, which contained (in mM): 115 NaCl, 5 KCl, 2 CaCl₂, 1 MgSO₄, 1.1 Na₂PO₄, 26 NaHCO₃, and 10 glucose; pH 7.4, when bubbled with 95% O₂ and 5% CO₂. Detached retinae were placed on a membrane filter (Millipore GSWP04700; Merck KGaA or ADVANTEC A045A013A; TOYO ROSHI KAISHA, LTD.) with the photoreceptor side up and sliced at a thickness of 150 μ m with a slicer (ST-20; Narishige). Sliced retinae were continuously perfused (3 ml/min) with oxygenated Ringer's solution during experiments. Temperature was maintained at 32–34°C. Slices were kept at room temperature in oxygenated Ringer's solution until used.

In some experiments (Figs. 3 and 4), recordings from ON SACs were performed using whole-mount preparations. To obtain whole-mount preparations, isolated retinae were cut into quarters and mounted ganglion cell-side-up over a 1-mm² hole in a filter paper. Data acquired from sliced retinae and whole-mount retinae were analyzed together.

Current recordings

Membrane currents were recorded from SACs identified by a GFP fluorescent signal when viewed under a fluorescent microscope (E600FN; Nikon or BX51WI; Olympus). ON and OFF SACs were identified from the location of their somas. Patch pipettes were pulled from borosilicate glass (Hilgenberg GmbH) using an electrode puller (P-97; Sutter Instrument or PP-83; Narishige). In whole-cell recordings from SACs, we used patch pipettes with a resistance of 8–12 M Ω when filled with an intrapipette solution, which contained (in mM): 135 KCl, 0.5 CaCl₂, 5 HEPES, 5 EGTA, 5 ATP-2Na, and 1 GTP-3Na. pH was adjusted to 7.2 with KOH. Under our experimental conditions, the equilibrium potential of Cl⁻ was +2.4 mV. Current signals were recorded with an Axopatch 200B amplifier (Molecular Devices), low-pass filtered at 5 kHz, and digitized at 10 kHz with a DigiData 1322A or 1550B interface controlled by pCLAMP software (RRID:SCR_011323; version 11). Drugs were applied to slices in the bath. Holding potentials corrected for liquid junction potentials were -65 mV.

Current analysis

Recorded signals were analyzed offline. Postsynaptic currents (PSCs) were automatically detected with a custom-written script in IGOR Pro (RRID:SCR_000325) using the threshold of "PSC amplitude," set at fivefold the SD of the baseline. The whole trace was then visualized to check for the over- or underdetection of events. "Likely" events were carefully inspected for the manual addition or deletion of the event. In the analysis of PSCs, 20-s analysis time windows were placed before (control) and during the application of pharmacological agents. The firing rate, average amplitude, and charge transfer within these windows were computed. When we detected slow baseline fluctuations, we excluded them and calculated the charge transfer.

To calculate the decay time constant (τ) of PSCs, we selected events that did not show any signs of multiple peaks (interevent

interval >50 ms) within analysis time windows. Events with rise times exceeding 1 ms were excluded because we were unable to establish whether this was attributed to dendritic filtering or the asynchronous overlap of events. Since the decay phase of individual PSCs was better fitted with a double-exponential function than a single-exponential function, we employed the former. The weighted decay time constant (τ_w) calculated from the double-exponential curve fit was used in the analysis.

Statistical analysis

Statistical analyses were performed using Origin 2023 (RRID: SCR_014212). The paired *t*-test was used for comparisons between two matched samples. A one-way ANOVA for repeated measures followed by Tukey's post hoc test was used for comparisons among three matched samples. In case of the violation of the sphericity assumption, the Greenhouse-Geisser correction was employed. P values < 0.05 were considered to be significant. All bar graphs and error bars represent means and SEM.

Results

ACh increased PSCs in SACs

SACs were identified by GFP labeling, and whole-cell currents were recorded from ON and OFF SACs. Unless otherwise specified, we used 2–3-wk-old mice because they are suitable for slice preparation. Following the application of ACh (100 μ M) to the bath, the frequency of PSCs significantly increased in ON (Fig. 1, B and C, left; P < 0.001) and OFF SACs (Fig. 1, D and E, left; P < 0.001). The average amplitude of PSCs was decreased by ACh in some cells (5/29 cells in ON SACs, 7/27 cells in OFF SACs), but significantly increased on average (ON SACs: Fig. 1 C, middle; P < 0.001; OFF SACs: Fig. 1 E, middle; P = 0.005). However, since many overlapping events were detected, precise calculations of the frequency and mean amplitude of PSCs were difficult. Therefore, we herein calculated the charge transfer to make an overall assessment of PSCs. The charge transfer was also significantly increased by ACh in ON (Fig. 1 C, right; P < 0.001) and OFF (Fig. 1 E, right; P < 0.001) SACs.

To compare the time course of PSCs before and after the application of ACh, we selected well-separated events (see Materials and methods) and calculated τ_w . The average τ_w of individual cells before and after the application of ACh was calculated when the number of selected PSCs during each recording condition was >3. In ON and OFF SACs, no significant change was observed in average τ_w before and after the application of ACh (ON SACs, P = 0.942; OFF SACs, P = 0.616, paired *t*-test). The mean \pm SEM of τ_w before and after the application of ACh calculated from the pooled average were 13.78 ± 0.80 and 13.86 ± 0.86 ms, respectively, for ON SACs ($n = 22$ cells from 19 mice), and 11.95 ± 0.83 ms and 12.39 ± 1.08 ms, respectively, for OFF SACs ($n = 25$ cells from 20 mice).

ACh-induced currents were blocked by SR95531

Consistent with our previous findings (Kaneda et al., 2008), the majority of spontaneous PSCs (sPSCs) were blocked by SR95531, a GABA_A receptor antagonist (30 μ M), in ON (Fig. 2, A and C; F(1.05, 7.34) = 18.83, P = 0.003, Ctrl versus SR, P < 0.001) and

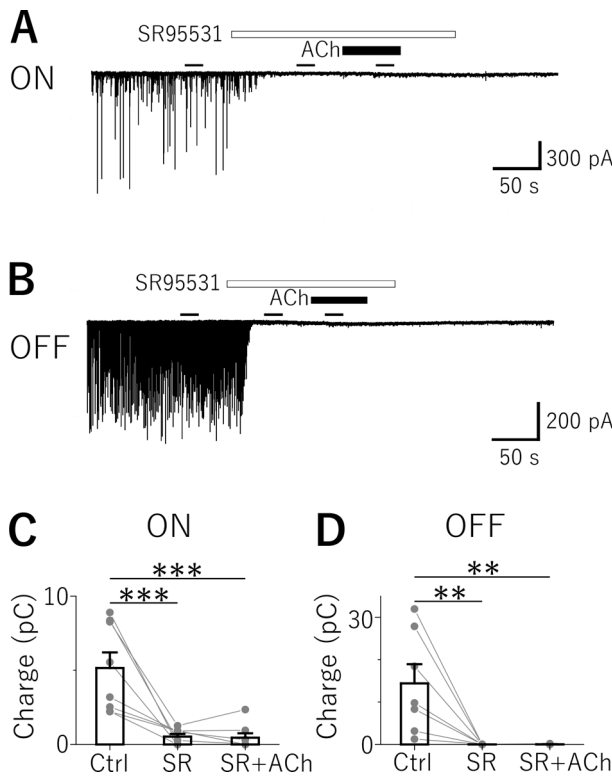


Figure 2. SR95531 blocked ACh-induced PSCs in SACs. (A and B) Effects of SR95531 on ACh-induced PSCs in ON SACs (A) and OFF SACs (B). The open bar above the trace shows the timing of the SR95531 application. Thick black bars show the timing of the ACh application. The thin black bars show the analysis time windows (20 s) of PSCs. (C and D) Summary of SR95531 effects on charge transfer in ON SACs (C: Ctrl versus SR, $P = 0.000324$; Ctrl versus SR + ACh, $P = 0.000281$; SR versus SR + ACh, $P = 0.996$; $n = 8$ cells from eight mice) and OFF SACs (D: Ctrl versus SR, $P = 0.00572$; Ctrl versus SR + ACh, $P = 0.00582$; SR versus SR + ACh, $P = 1.000$; $n = 7$ cells from five mice). Ctrl, before drug application; SR, during the SR95531 application; SR + ACh, during the ACh application in the presence of SR95531. A one-way repeated measures ANOVA and Tukey's post hoc test were used. ** $P < 0.01$, *** $P < 0.001$.

OFF (Fig. 2, B and D; $F(1.00, 6.00) = 10.02$, $P = 0.019$, Ctrl versus SR, $P = 0.006$) SACs, indicating that they were GABAergic. In the presence of SR95531, the application of ACh did not significantly increase PSCs in ON (Fig. 2 C; SR versus SR + ACh, $P = 0.996$) or OFF (Fig. 2 D; SR versus SR + ACh, $P = 1.000$) SACs. Under this condition, we did not detect any apparent slow inward currents in ON or OFF SACs, confirming previous findings showing that SACs themselves did not respond to ACh after eye-opening (Zheng et al., 2004). Therefore, ACh acted on ACh receptors located on GABAergic neurons presynaptic to ON and OFF SACs.

Distinct ACh receptors mediate ACh-induced currents between young and adult mice

To identify the subtypes of ACh receptors mediating ACh-induced GABAergic PSCs in SACs, we examined the effects of nicotine (100 μ M), a nicotinic ACh receptor agonist, and oxotremorine (100 μ M), a muscarinic ACh receptor agonist.

In P7–8 mice, nicotine significantly increased the charge transfer of PSCs in ON (Fig. 3 A left, B left; $P = 0.005$) and OFF (Fig. 3 C left, D left; $P = 0.007$) SACs, whereas oxotremorine did

not in ON (Fig. 3 A right, B right; $P = 0.276$) or OFF (Fig. 3 C right, D right; $P = 0.604$) SACs. The bath application of nicotine-induced slow inward currents resulted in a baseline deflection in ON SACs (Fig. 3 A left). Even when synaptic inputs were blocked by 100 μ M CdCl₂ or by a cocktail containing 10 μ M 6-cyano-7-nitroquinoxaline-2,3-dione (CNQX, an AMPA/kainate receptor antagonist), 50 μ M D-(–)-2-amino-5-phosphonopentanoic acid (D-AP5, an NMDA receptor antagonist), 1 μ M strychnine (a glycine receptor antagonist), and 2 μ M SR95531, slow inward currents were observed (average amplitude: 57.86 \pm 11.71 pA, $n = 5$ ON SACs), indicating the existence of ACh receptors on SACs prior to eye-opening, as shown in a previous study (Zheng et al., 2004). These inward currents were also observed in OFF SACs (Fig. 3 C left) but were smaller than those in ON SACs. Even under the condition where synaptic inputs were blocked, inward currents were induced by nicotine in OFF SACs (average amplitude: 29.43 \pm 9.71 pA, $n = 6$ OFF SACs).

The effects of oxotremorine in adult mice (\geq P28) differed from those in P7–8 mice. In adult mice, nicotine again increased the charge transfer of PSCs in ON (Fig. 4 A left, B left; $P = 0.018$) and OFF SACs (Fig. 4 C left, D left; $P < 0.001$). Unexpectedly, oxotremorine increased the charge transfer of PSCs in ON SACs (Fig. 4 A right, B right; $P = 0.010$), while it had no effect in OFF SACs (Fig. 4 C right, D right; $P = 0.740$). These results suggested the involvement of either a new set of receptors on the same population of presynaptic GABAergic amacrine cells or a new population of amacrine cells with GABAergic inputs to ON SACs.

Tetrodotoxin (TTX) did not block ACh-induced currents in SACs

The GABAergic neurons making synaptic contacts in the IPL are members of a heterogeneous population of amacrine cells (Zhang and McCall, 2012). The present results showed that SACs received GABAergic inputs from neighboring amacrine cells. Since amacrine cells are classified into spiking cells (e.g., poly-axonal amacrine cells, monkey [Greschner et al., 2014]; rabbit [Völgyi et al., 2001]; mouse [Sabbah et al., 2017]) and non-spiking cells (e.g., SACs, mouse [Ozaita et al., 2004; Kaneda et al., 2007]; rabbit [Taylor and Wässle, 1995]), we investigated whether the application of TTX (1 μ M), a voltage-gated Na⁺ channel blocker, inhibited the effects of ACh. In ON SACs, the application of TTX did not affect the charge transfer of sPSCs (Fig. 5, A and C; $F(1.09, 5.45) = 9.01$, $P = 0.026$, Ctrl versus TTX, $P = 0.986$), but decreased it in OFF SACs (Fig. 5, B and D; $F(2, 10) = 11.81$, $P = 0.002$, Ctrl versus TTX, $P = 0.011$). In the presence of TTX, the application of ACh increased the charge transfer of PSCs in ON (Fig. 5, A and C; TTX versus TTX + ACh, $P = 0.010$) and OFF (Fig. 5, B and D; TTX versus TTX + ACh, $P = 0.003$) SACs. These results indicate that ON and OFF SACs receive ACh-mediated GABAergic inputs from non-spiking amacrine cells.

The mGluR2 receptor agonist LY354740 did not block ACh-induced currents in SACs

Since SACs are non-spiking amacrine cells (Ozaita et al., 2004; Kaneda et al., 2007) and reciprocal GABAergic synapses are formed between SACs (Zheng et al., 2004), we investigated whether the release of GABA onto the dendrites of SACs was

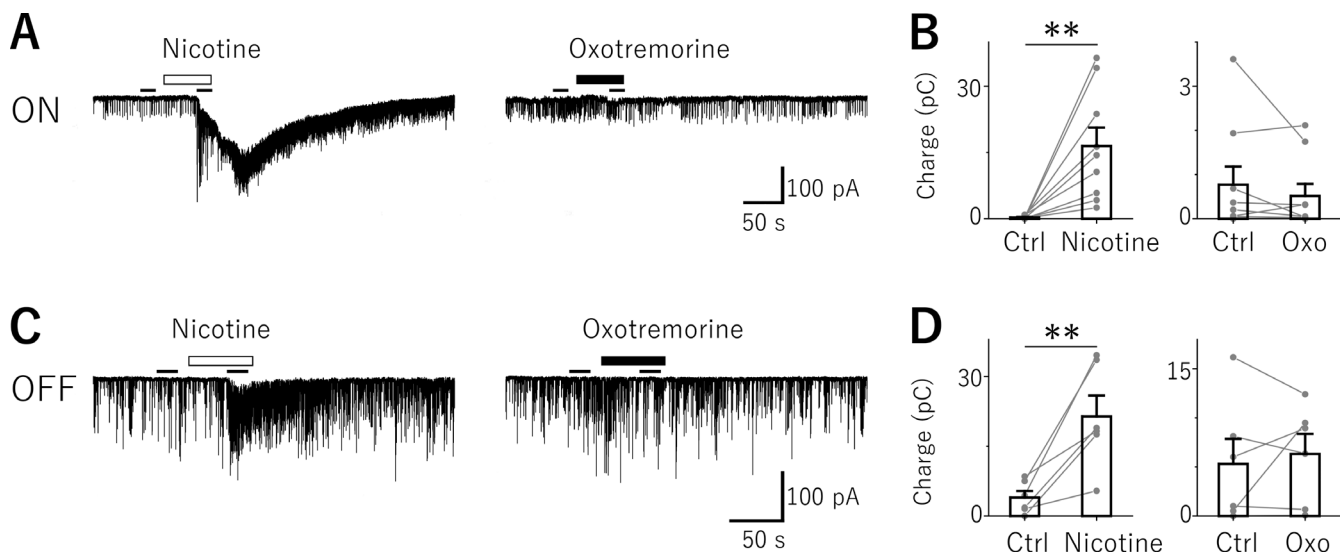


Figure 3. A nicotinic agonist increased PSCs in SACs in young (P7-8) mice. (A and C) Responses to nicotine (left) and oxotremorine (right) in ON SACs (A) and OFF SACs (C). The open bar above the trace shows the timing of the nicotine application. The thick black bar shows the timing of the oxotremorine application. Thin black bars indicate the analysis time windows (20 s) of PSCs. **(B and D)** Summary of the effects of nicotine (left) and oxotremorine (Oxo, right) on the charge transfer of ON SACs (B: nicotine, $P = 0.00484$; Oxo, $P = 0.276$, $n = 9$ cells [two from sliced retinae, 7 from whole-mount retinae] of six mice) and OFF SACs (D: nicotine, $P = 0.00733$; Oxo, $P = 0.604$, $n = 6$ cells [all from the sliced retinae] of four mice). Ctrl, before drug application; nicotine, during the nicotine application; Oxo, during the oxotremorine application. A paired *t*-test was used. ** $P < 0.01$. Nicotine and oxotremorine were applied to the same cell in the order of oxotremorine followed by nicotine. Recordings were performed on P7-8 mice.

mediated by the effects of ACh on neighboring SACs by blocking reciprocal synapses with the mGluR2 agonist, LY354740. mGluR2 agonists were previously reported to inhibit voltage-gated calcium channels in SACs (Koren et al., 2017), abolish

neurotransmitter release from SACs (Sethuramanujam et al., 2018), and reduce the directional selectivity of ganglion cells by enhancing their null spiking response (Jensen, 2006). In ON and OFF SACs, 1 μ M LY354740 did not block ACh-induced PSCs

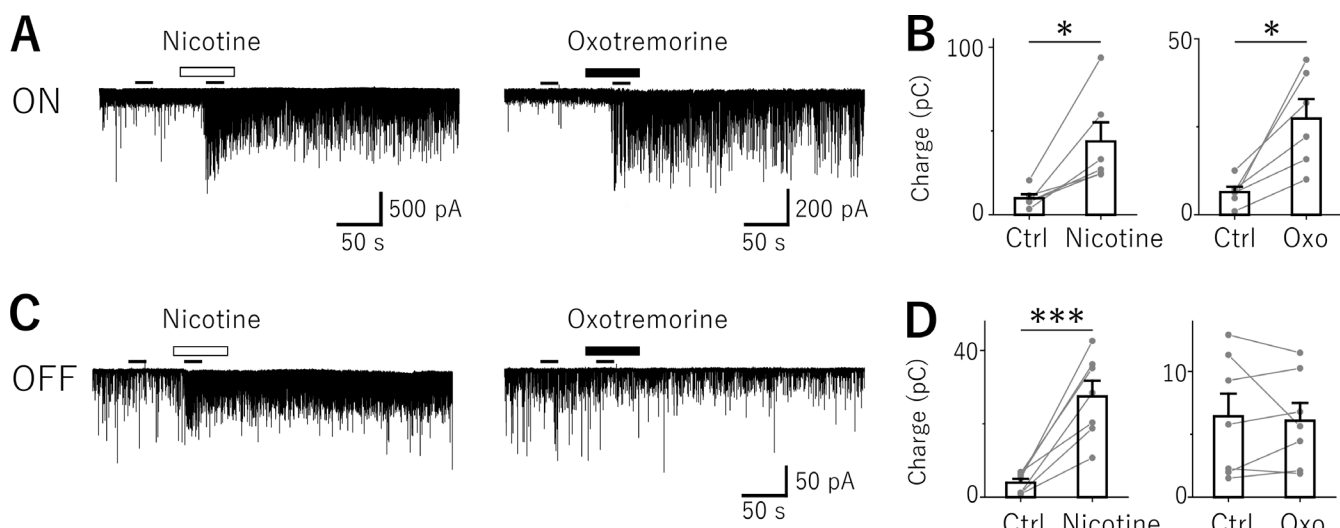


Figure 4. In adult mice ($\geq P28$), not only a nicotinic agonist, but also a muscarinic agonist increased PSCs in ON SACs. (A and C) Responses to nicotine (left) and oxotremorine (right) in ON SACs (A) and OFF SACs (C). The open bar above the trace shows the timing of the nicotine application. The thick black bar shows the timing of the oxotremorine application. Thin black bars show the analysis time windows (20 s) of PSCs. **(B and D)** Summary of the effects of nicotine (left) and oxotremorine (Oxo, right) on the charge transfer of ON SACs (B: nicotine, $P = 0.0176$, $n = 6$ cells [all from the whole-mount retinae] of five mice; Oxo, $P = 0.0101$, $n = 6$ cells [all from the whole-mount retinae] of five mice) and OFF SACs (D: Nicotine, $P = 0.000811$; Oxo, $P = 0.739$, $n = 7$ cells [six from sliced, one from whole-mount retinae] of five mice). Ctrl, before drug application; nicotine, during the nicotine application; Oxo, during the oxotremorine application. A paired *t*-test was used. * $P < 0.05$, ** $P < 0.01$, *** $P < 0.001$. Oxotremorine and nicotine were applied to different cells in ON SACs because the effects of oxotremorine persisted for a long time. Nicotine and oxotremorine were applied to the same cell in OFF SACs in the order of oxotremorine followed by nicotine. Recordings were performed on adult mice ($\geq P28$).

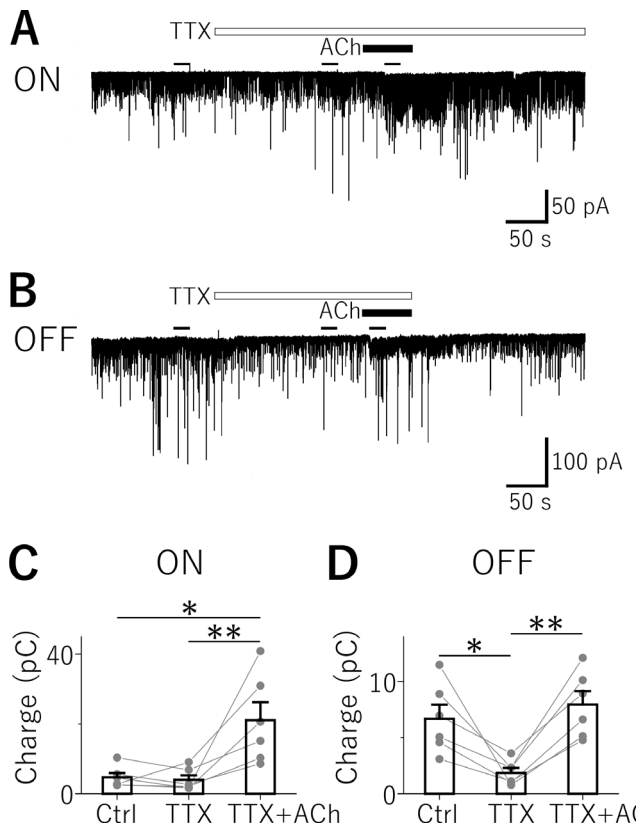


Figure 5. ACh-induced PSCs were mediated by non-spiking amacrine cells. (A and B) Effects of TTX on ACh-induced PSCs in an ON SAC (A) and an OFF SAC (B). Open bars above the trace show the timing of the TTX application. Thick black bars show the timing of the ACh application. Thin black bars show the analysis time windows (20 s) of PSCs. **(C and D)** Summary of the effects of TTX on the charge transfer of ON SACs (C: Ctrl versus TTX, $P = 0.986$; Ctrl versus TTX + ACh, $P = 0.0124$; TTX versus TTX + ACh, $P = 0.0096$, $n = 6$ cells from six mice) and OFF SACs (D: Ctrl versus TTX, $P = 0.0114$; Ctrl versus TTX + ACh, $P = 0.615$; TTX versus TTX + ACh, $P = 0.00253$, $n = 6$ cells from five mice). Ctrl, before drug application; TTX, during the TTX application; TTX + ACh, during the ACh application in the presence of TTX. A one-way repeated measures ANOVA and Tukey's post hoc test were used. * $P < 0.05$, ** $P < 0.01$.

in SACs (ON SACs: **Fig. 6, A and C**; $F(1.04, 7.29) = 7.10$, $P = 0.030$, LY versus LY + ACh, $P = 0.007$; OFF SACs: **Fig. 6, B and D**; $F(2, 10) = 50.57$, $P < 0.001$, LY versus LY + ACh, $P < 0.001$), suggesting that ON and OFF SACs receive ACh-mediated inputs from GABAergic amacrine cells other than SACs. However, the charge transfer of sPSCs was significantly reduced by LY354740 in OFF SACs (**Fig. 6 D**; Ctrl versus LY, $P = 0.016$), indicating that neighboring SACs release GABA, similar to the rabbit retina ([Zheng et al., 2004](#)) at rest. In ON SACs, although the charge transfer of sPSCs was decreased in all cells (8/8 cells) by LY354740, the reduction was not significant (**Fig. 6 C**; Ctrl versus LY, $P = 0.665$), which may have been due to the smaller charge transfer of sPSCs in ON SACs than in OFF SACs.

Discussion

In the present study, we demonstrate that ACh increased GABAergic PSCs in ON and OFF SACs. ACh acted on nicotinic ACh

receptors in young (P7–8) and adult mice. In ON SACs, ACh also acted on muscarinic ACh receptors in adult mice. ON and OFF SACs both receive GABAergic inputs from TTX-insensitive cells. The present results indicate that ACh activated the GABAergic feedback system at the SAC level in the ON and OFF pathways. In addition, this GABAergic inhibition was controlled by the different subtypes of ACh receptors. SACs are currently known to contribute to the formation of direction selectivity ([Yoshida et al., 2001; Amthor et al., 2002; Vlasits et al., 2014](#)). GABAergic inputs from SACs to direction-selective RGCs are important for the formation of direction selectivity ([Taylor et al., 2000; Fried et al., 2002; Lee et al., 2010; Wei et al., 2011; Pei et al., 2015](#)). On the other hand, the functional role of ACh remains unclear. Since SACs are the only ACh-releasing neurons in the retina, these results imply a negative feedback loop in which ACh released by SACs activates pre-synaptic GABAergic neurons to inhibit SACs. The significance of nicotinic versus muscarinic +

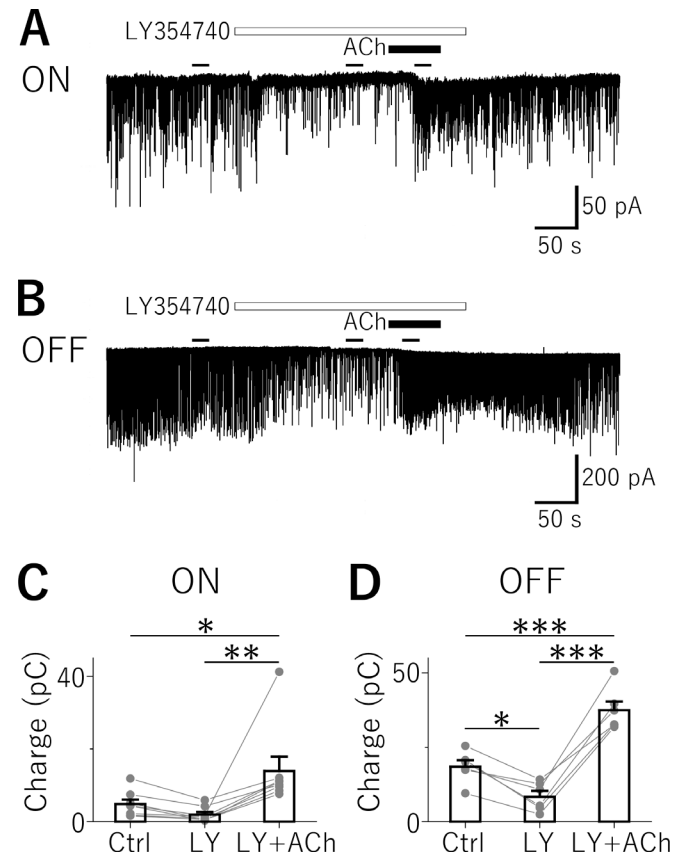


Figure 6. ACh-induced PSCs were mediated by amacrine cells other than SACs. (A and B) Effects of LY354740 on ACh-induced PSCs in an ON SAC (A) and an OFF SAC (B). Open bars above the trace show the timing of the LY354740 application. Thick black bars show the timing of the ACh application. Thin black bars show the analysis time windows (20 s) of PSCs. **(C and D)** Summary of the effects of LY354740 on the charge transfer of ON SACs (C: Ctrl versus LY, $P = 0.665$; Ctrl versus LY + ACh, $P = 0.0400$; LY versus LY + ACh, $P = 0.00749$, $n = 8$ cells from four mice) and OFF SACs (D: Ctrl versus LY, $P = 0.0156$; Ctrl versus LY + ACh, $P = 0.000196$; LY versus LY + ACh, $P = 4.68 \times 10^{-6}$, $n = 6$ cells from five mice). Ctrl, before drug application; LY, during the LY354740 application; LY + ACh, during the ACh application in the presence of LY354740. A one-way repeated measures ANOVA and Tukey's post hoc test were used. * $P < 0.05$, ** $P < 0.01$, *** $P < 0.001$.

muscarinic feedback is more difficult to rationalize. We speculate that if the effects of ACh release are local, these receptors may be located on the presynaptic terminals themselves.

Types of synaptic inputs to SACs

Consistent with previous findings (Kaneda et al., 2008), the application of SR95531 abolished the majority of sPSCs in both ON and OFF SACs. Furthermore, ACh did not induce any increase in PSCs in the presence of SR95531, suggesting that the majority of sPSCs and ACh-induced PSCs in SACs were GABAergic. However, we noted that a few residual responses persisted after the blockade of GABA_A receptors. These residual responses may be excitatory glutamatergic inputs, as indicated by a previous study (Petit-Jacques et al., 2005). Bipolar cells presynaptic to SACs have been reported to express nicotinic receptors (Hall et al., 2019; Hellmer et al., 2021), implying that ACh may increase glutamatergic inputs onto SACs. However, this is not likely to be the case because ACh did not significantly increase PSCs in the presence of SR95531. Nevertheless, the possibility of ACh increasing glutamatergic inputs onto SACs cannot be entirely ruled out. The smaller amplitudes and faster decay kinetics than those of GABAergic PSCs (Frech et al., 2001) posed challenges in distinguishing glutamatergic inputs from baseline noise. In addition, we need to consider the shunting of excitatory inputs toward the centripetal direction by the large K⁺ conductance at the proximal portion of the dendrites of SACs (Ozaita et al., 2004).

Although glycinergic sPSCs have been detected in ON SACs (Majumdar et al., 2009; Jain et al., 2022), we did not identify distinct inhibitory PSCs following the application of SR95531 as we have previously reported (Kaneda et al., 2008). This discrepancy may be attributed to the slowest τ value among retinal amacrine cells (Majumdar et al., 2009), likely due to the prominent expression of the glycine receptor $\alpha 4$ subunit in ON SACs (Heinze et al., 2007; Majumdar et al., 2009; Jain et al., 2022), smaller amplitudes than GABAergic sPSCs (Jain et al., 2022), or tonic glycinergic inputs that ON SACs may receive (Majumdar et al., 2009). Therefore, further studies on the effects of ACh on glycinergic inputs are needed.

Inputs from spiking amacrine cells

In OFF SACs, the application of TTX significantly decreased sPSCs, indicating a constant GABAergic input from spiking amacrine cells in a steady state. Alternatively, it is possible that OFF SACs receive GABAergic inputs from amacrine cells, which primarily receive glutamatergic inputs from bipolar cells expressing Na⁺ channels (Hellmer et al., 2016). On the other hand, TTX had no effect on sPSCs in ON SACs, indicating the absence of constant input from those amacrine cells. These results support ON and OFF SACs being regulated by distinct networks of amacrine cells.

In ON SACs, the application of ACh increased the charge transfer of PSCs even in the presence of TTX, similar to the TTX-free condition. This result strongly suggests the involvement of non-spiking amacrine cells in ACh-induced GABAergic inputs to ON SACs. Similarly, in OFF SACs, ACh increased the charge transfer of PSCs in the presence of TTX, confirming the

involvement of non-spiking amacrine cells in ACh-induced GABAergic inputs to OFF SACs. However, as shown in Fig. 5 D, the amount of charge transfer during the application of ACh (TTX + ACh) was similar to that before the application of TTX (Ctrl). Since an increase in the amount of charge transfer by ACh has been observed in the absence of TTX in OFF SACs (Fig. 1 E), the reduction in the amount of charge transfer by ACh recorded in the presence of TTX may result from the loss of constant GABAergic inputs from spiking amacrine cells and/or the loss of ACh-induced GABAergic inputs from spiking amacrine cells. In any case, further studies are needed to establish whether spiking amacrine cells also contribute to ACh-induced GABAergic inputs to OFF SACs.

Types of presynaptic amacrine cells to SACs

The present results showed that ON and OFF SACs received GABAergic inputs driven by ACh receptors. These ACh-induced GABAergic inputs persisted after spiking amacrine cells were blocked by TTX. In addition, the blocking of reciprocal synapses between SACs by LY354740 (Koren et al., 2017; Sethuramanujam et al., 2018) did not inhibit ACh-induced GABAergic inputs onto SACs. These results indicate that non-spiking amacrine cells other than SACs formed GABAergic synaptic contacts on SACs (Fig. 7). In the rabbit retina, SACs form GABAergic reciprocal synapses between them but have no cholinergic reciprocal synapses after eye opening (Zheng et al., 2004), which confirmed that GABAergic reciprocal synapses were not driven by cholinergic inputs from SACs after eye-opening.

It currently remains unclear whether GABAergic amacrine cells, presynaptic to SACs, directly receive ACh from SACs. Recent studies highlighted the effects of ACh on bipolar cell terminals (Hall et al., 2019; Hellmer et al., 2021; Matsumoto et al., 2021). These findings suggest that ACh-induced GABAergic inputs in SACs may originate from amacrine cells indirectly activated by ACh via bipolar cells that express nicotinic receptors.

The classification of amacrine cells has been challenged by many researchers and many subtypes are classified by their morphological characteristics in the mouse retina (Gustincich et al., 1997; Badea and Nathans, 2004; Lin and Masland, 2006; Pérez De Sevilla Müller et al., 2007; Majumdar et al., 2009; Pang et al., 2012). Furthermore, a connectomic reconstruction revealed the presence of 45 types of amacrine cells (Helmstaedter et al., 2013). The high-level heterogeneity of amacrine cells has been supported by findings obtained using high-throughput single-cell RNA sequencing, which identified 63 types of amacrine cells, containing 43 types of GABAergic cells (Yan et al., 2020). Since narrow-field amacrine cells are glycinergic (Menger et al., 1998) and axon-bearing (polyaxonal) wide-field amacrine cells displayed somatic action potentials (Völgyi et al., 2001), axonless medium- or wide-field amacrine cells with dendrites in the same layer as SACs may be candidate amacrine cells that provide ACh-induced GABAergic inputs to SACs. Referencing the study conducted by Ding et al. (2016), which showed several wide-field ACs presynaptic to SACs, and considering the comprehensive dataset presented by Helmstaedter et al. (2013), the prospective amacrine cell candidates for OFF SACs may be types 55–57, while those for ON SACs may be types

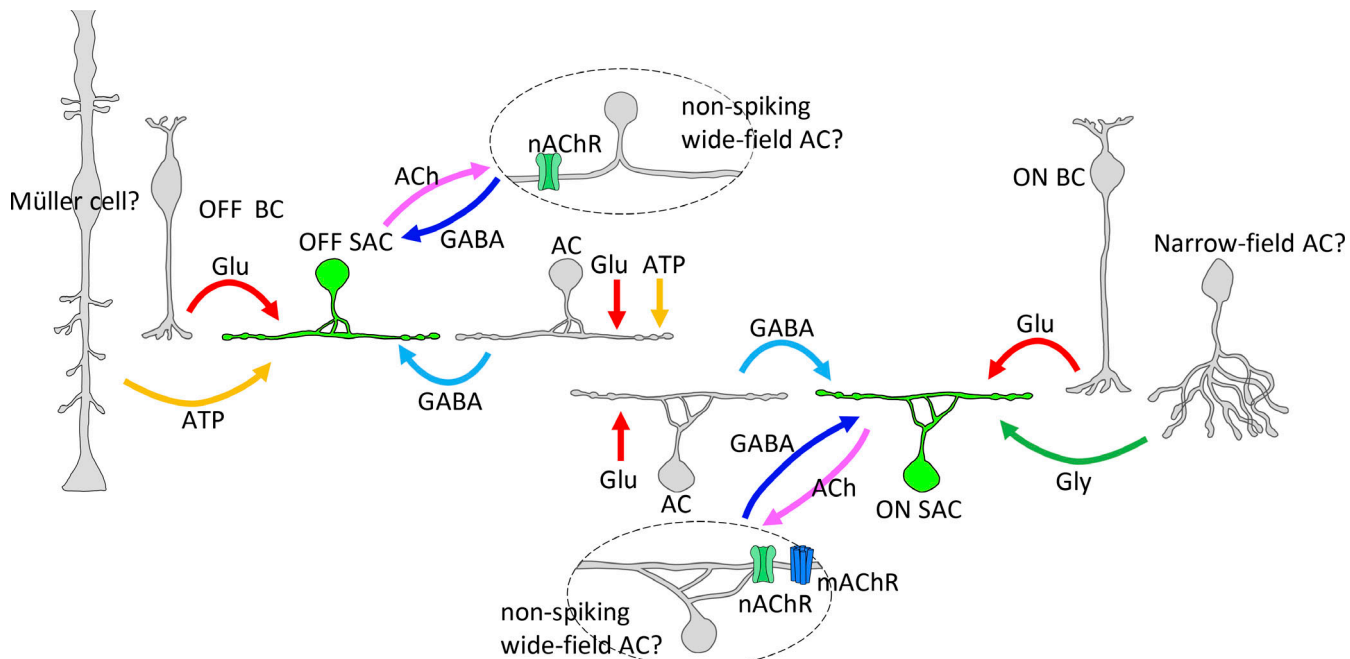


Figure 7. ON and OFF SACs receive distinct synaptic inputs. Schematic drawing of synaptic wiring in ON and OFF SACs (green cells) in the adult mouse retina. ON and OFF SACs both receive nicotinic receptor-mediated GABAergic inputs (blue) and only ON SACs receive additional muscarinic receptor-mediated GABAergic inputs (blue). These cholinergic receptors presumably exist in non-spiking amacrine cells other than SACs (cells surrounded by dotted lines). OFF SACs, but not ON SACs, have P2X₂ purinoreceptors and respond to ATP (yellow) (Kaneda et al., 2008). ATP also activates P2X purinoreceptors on amacrine cells (OFF SACs are a likely candidate) and increases GABAergic inputs (light blue) to OFF SACs. ON SACs selectively receive glycinergic inputs (green), presumably from narrow-field amacrine cells (Ishii and Kaneda, 2014). Canonical glutamatergic inputs (red) from bipolar cells (BC) are also shown. This glutamatergic circuit drives GABAergic inputs (light blue) to both ON and OFF SACs from neighboring amacrine cells (Ishii and Kaneda, 2014). Glu, glutamate; Gly, glycine; BC, bipolar cell; AC, amacrine cell; nAChR, nicotinic acetylcholine receptor; mAChR, muscarinic acetylcholine receptor.

28, 30, and 32 of Helmsteader's dataset. Regarding ON SACs, we demonstrated that muscarinic receptors were involved in GABAergic feedback to ON SACs in adults. Single-cell RNA sequencing showed that muscarinic receptors were selectively expressed in some GABAergic amacrine cells (Yan et al., 2020). If GABAergic amacrine cells directly receive ACh from SACs, we will be able to narrow down candidate amacrine cells that provide ACh-induced GABAergic inputs to ON SACs when further morphological information on muscarinic receptor-expressing amacrine cells is available.

Distinctions between ON and OFF pathways

We showed that different ACh receptors regulated GABAergic inputs to ON and OFF SACs in adults, indicating that synaptic wiring is distinct between ON and OFF SACs. This concept is further supported by TTX-sensitive GABAergic inhibition only being observed in OFF SACs.

Different synaptic wiring between ON and OFF SACs has been reported. We observed significantly larger responses to glycine in ON SACs than in OFF SACs (Ishii and Kaneda, 2014) and significantly larger responses to ATP in OFF SACs than in ON SACs (Kaneda et al., 2004, 2008) (Fig. 7). The study investigating differences in light responses between ON and OFF SACs revealed that the blockage of NMDA receptors significantly shortened the duration of proximal excitation in OFF SACs but not in ON SACs (Fransen and Borghuis, 2017). Regarding functional differences in inhibitory inputs to ON and OFF SACs,

inhibitory inputs from other amacrine cells were not necessary for the direction selectivity of ON SACs, while feed-forward inhibition from non-SAC amacrine cells contributed to the direction selectivity of OFF SACs (Chen et al., 2016). Distinctions between the ON and OFF pathways have also been reported at the ganglion cell level. In direction-selective RGC, the directional difference in the total inhibitory input was larger for ON responses than for OFF responses (Taylor and Vaney, 2002). Moreover, Fried et al. (2005) reported that curare, a blocker of nicotinic ACh receptors, reduced the directionality of inhibitory inputs to direction-selective RGCs in a different manner between ON and OFF responses. The brain does not respond equally to increments and decrements in light (Zemon et al., 1988; Chubb et al., 2004). Therefore, even among mirror-symmetric pairs, it is plausible that ON and OFF types undergo distinct regulatory processes.

In the present study, we found that GABAergic inputs to SACs were regulated by ACh. In rod bipolar cells, GABAergic inputs from A17 amacrine cells were also regulated by ACh (Elgueta et al., 2015). In the rabbit retina, nicotinic agonists were reported to increase the release of GABA, consequently leading to an indirect increase in dopamine release (Neal et al., 2001). Collectively, the present results and these findings suggest that ACh functions as an indirect inhibitory transmitter through GABAergic systems in the retina. The functional role of ACh in the retina needs to be reconsidered from both its direct effects on RGCs and its indirect inhibition at multiple levels.

Data availability

Data for all figures will be made available upon reasonable request to the corresponding author.

Acknowledgments

Christopher J. Lingle served as editor.

We thank Dr. Ikuo Ogiwara for his fruitful discussions and suggestions. We also thank Chiaki Suzuki for her technical assistance.

This work was supported by JSPS KAKENHI (Grant numbers JP22K18162 to M. Gangi, JP23K14303 to T. Maruyama, JP22K09823 to T. Ishii, and JP20K09836 to M. Kaneda) and by a Nippon Medical School Grant-in-Aid for Medical Research (to M. Kaneda).

Author contributions: M. Gangi: Conceptualization, Data curation, Formal analysis, Funding acquisition, Investigation, Resources, Software, Validation, Writing—original draft, T. Maruyama: Data curation, Formal analysis, Investigation, Methodology, Validation, Writing—original draft, T. Ishii: Conceptualization, Formal analysis, Funding acquisition, Investigation, Methodology, Project administration, Supervision, Validation, Writing—review and editing, M. Kaneda: Conceptualization, Data curation, Formal analysis, Funding acquisition, Investigation, Methodology, Project administration, Resources, Supervision, Validation, Writing—original draft.

Disclosures: The authors declare no competing interests exist.

Submitted: 8 February 2024

Revised: 19 April 2024

Accepted: 27 May 2024

References

Amthor, F.R., K.T. Keyser, and N.A. Dmitrieva. 2002. Effects of the destruction of starburst-cholinergic amacrine cells by the toxin AF64A on rabbit retinal directional selectivity. *Vis. Neurosci.* 19:495–509. <https://doi.org/10.1017/S0952523802194119>

Ariel, M., and N.W. Daw. 1982. Pharmacological analysis of directionally sensitive rabbit retinal ganglion cells. *J. Physiol.* 324:161–185. <https://doi.org/10.1113/jphysiol.1982.sp014105>

Badea, T.C., and J. Nathans. 2004. Quantitative analysis of neuronal morphologies in the mouse retina visualized by using a genetically directed reporter. *J. Comp. Neurol.* 480:331–351. <https://doi.org/10.1002/cne.20304>

Briggman, K.L., M. Helmstaedter, and W. Denk. 2011. Wiring specificity in the direction-selectivity circuit of the retina. *Nature*. 471:183–188. <https://doi.org/10.1038/nature09818>

Brombas, A., S. Kalita-de Croft, E.J. Cooper-Williams, and S.R. Williams. 2017. Dendro-dendritic cholinergic excitation controls dendritic spike initiation in retinal ganglion cells. *Nat. Commun.* 8:15683. <https://doi.org/10.1038/ncomms15683>

Chen, Q., Z. Pei, D. Koren, and W. Wei. 2016. Stimulus-dependent recruitment of lateral inhibition underlies retinal direction selectivity. *Elife*. 5: 1–19. <https://doi.org/10.7554/elife.21053>

Chiao, C.-C., and R.H. Masland. 2002. Starburst cells nondirectionally facilitate the responses of direction-selective retinal ganglion cells. *J. Neurosci.* 22:10509–10513. <https://doi.org/10.1523/JNEUROSCI.22-24-10509.2002>

Chubb, C., M.S. Landy, and J. Economou. 2004. A visual mechanism tuned to black. *Vis. Res.* 44:3223–3232. <https://doi.org/10.1016/j.visres.2004.07.019>

Cohen, E.D., and R.F. Miller. 1995. Quinoxalines block the mechanism of directional selectivity in ganglion cells of the rabbit retina. *Proc. Natl. Acad. Sci. USA*. 92:1127–1131. <https://doi.org/10.1073/pnas.92.4.1127>

Ding, H., R.G. Smith, A. Poleg-Polsky, J.S. Diamond, and K.L. Briggman. 2016. Species-specific wiring for direction selectivity in the mammalian retina. *Nature*. 535:105–110. <https://doi.org/10.1038/nature18609>

Elgueta, C., A.H. Vielma, A.G. Palacios, and O. Schmachtenberg. 2015. Acetylcholine induces GABA release onto rod bipolar cells through heteromeric nicotinic receptors expressed in A17 amacrine cells. *Front. Cell. Neurosci.* 9:6. <https://doi.org/10.3389/fncel.2015.00006>

Famiglietti, E.V.Jr. 1983. “Starburst” amacrine cells and cholinergic neurons: Mirror-symmetric on and off amacrine cells of rabbit retina. *Brain Res.* 261:138–144. [https://doi.org/10.1016/0006-8993\(83\)91293-3](https://doi.org/10.1016/0006-8993(83)91293-3)

Famiglietti, E.V.Jr., A. Kaneko, and M. Tachibana. 1977. Neuronal architecture of on and off pathways to ganglion cells in carp retina. *Science*. 198: 1267–1269. <https://doi.org/10.1126/science.73223>

Famiglietti, E.V.Jr., and H. Kolb. 1976. Structural basis for ON-and OFF-center responses in retinal ganglion cells. *Science*. 194:193–195. <https://doi.org/10.1126/science.959847>

Fransen, J.W., and B.G. Borghuis. 2017. Temporally diverse excitation generates direction-selective responses in ON- and OFF-type retinal starburst amacrine cells. *Cell Rep.* 18:1356–1365. <https://doi.org/10.1016/j.celrep.2017.01.026>

Frech, M.J., J. Pérez-León, H. Wässle, and K.H. Backus. 2001. Characterization of the spontaneous synaptic activity of amacrine cells in the mouse retina. *J. Neurophysiol.* 86:1632–1643. <https://doi.org/10.1152/jn.2001.86.4.1632>

Fried, S.I., T.A. Münch, and F.S. Werblin. 2002. Mechanisms and circuitry underlying directional selectivity in the retina. *Nature*. 420:411–414. <https://doi.org/10.1038/nature01179>

Fried, S.I., T.A. Münch, and F.S. Werblin. 2005. Directional selectivity is formed at multiple levels by laterally offset inhibition in the rabbit retina. *Neuron*. 46:117–127. <https://doi.org/10.1016/j.neuron.2005.02.007>

Greschner, M., G.D. Field, P.H. Li, M.L. Schiff, J.L. Gauthier, D. Ahn, A. Sher, A.M. Litke, and E.J. Chichilnisky. 2014. A polyaxonal amacrine cell population in the primate retina. *J. Neurosci.* 34:3597–3606. <https://doi.org/10.1523/JNEUROSCI.3359-13.2014>

Grzywacz, N.M., F.R. Amthor, and D.K. Merwine. 1998a. Necessity of acetylcholine for retinal directionally selective responses to drifting gratings in rabbit. *J. Physiol.* 512:575–581. <https://doi.org/10.1111/j.1469-7793.1998.575be.x>

Grzywacz, N.M., D.K. Merwine, and F.R. Amthor. 1998b. Complementary roles of two excitatory pathways in retinal directional selectivity. *Vis. Neurosci.* 15:1119–1127. <https://doi.org/10.1017/S0952523898156109>

Gustincich, S., A. Feigenspan, D.K. Wu, L.J. Koopman, and E. Raviola. 1997. Control of dopamine release in the retina: A transgenic approach to neural networks. *Neuron*. 18:723–736. [https://doi.org/10.1016/S0896-6273\(00\)80313-X](https://doi.org/10.1016/S0896-6273(00)80313-X)

Hall, L.M., C.B. Hellmer, C.C. Koehler, and T. Ichinose. 2019. Bipolar cell type-specific expression and conductance of alpha-7 nicotinic acetylcholine receptors in the mouse retina. *Invest. Ophthalmol. Vis. Sci.* 60:1353–1361. <https://doi.org/10.1167/iovs.18-25753>

He, S., and R.H. Masland. 1997. Retinal direction selectivity after targeted laser ablation of starburst amacrine cells. *Nature*. 389:378–382. <https://doi.org/10.1038/38723>

Heinze, L., R.J. Harvey, S. Haverkamp, and H. Wässle. 2007. Diversity of glycine receptors in the mouse retina: Localization of the $\alpha 4$ subunit. *J. Comp. Neurol.* 500:693–707. <https://doi.org/10.1002/cne.21201>

Hellmer, C.B., Y. Zhou, B. Fyk-Kolodziej, Z. Hu, and T. Ichinose. 2016. Morphological and physiological analysis of type-5 and other bipolar cells in the Mouse Retina. *Neuroscience*. 315:246–258. <https://doi.org/10.1016/j.neuroscience.2015.12.016>

Hellmer, C.B., L.M. Hall, J.M. Bohl, Z.J. Sharpe, R.G. Smith, and T. Ichinose. 2021. Cholinergic feedback to bipolar cells contributes to motion detection in the mouse retina. *Cell Rep.* 37:110106. <https://doi.org/10.1016/j.celrep.2021.110106>

Helmstaedter, M., K.L. Briggman, S.C. Turaga, V. Jain, H.S. Seung, and W. Denk. 2013. Connectomic reconstruction of the inner plexiform layer in the mouse retina. *Nature*. 500:168–174. <https://doi.org/10.1038/nature12346>

Ikeda, H., and M.J. Sheardown. 1982. Acetylcholine may be an excitatory transmitter mediating visual excitation of “transient” cells with the periphery effect in the cat retina. Iontophoretic studies in vivo. *Neuroscience*. 7:1299–1308. [https://doi.org/10.1016/0306-4522\(82\)91135-6](https://doi.org/10.1016/0306-4522(82)91135-6)

Ishii, T., K. Homma, A. Mano, T. Akagi, Y. Shigematsu, Y. Shimoda, H. Inoue, Y. Kakinuma, and M. Kaneda. 2017. Novel channel-mediated choline transport in cholinergic neurons of the mouse retina. *J. Neurophysiol.* 118:1952–1961. <https://doi.org/10.1152/jn.00506.2016>

Ishii, T., and M. Kaneda. 2014. ON-pathway-dominant glycinergic regulation of cholinergic amacrine cells in the mouse retina. *J. Physiol.* 592: 4235–4245. <https://doi.org/10.1113/jphysiol.2014.271148>

Jain, V., L. Hanson, S. Sethuramanujam, T. Michaels, J. Gawley, R.G. Gregg, I. Pyle, C. Zhang, R.G. Smith, D. Berson, et al. 2022. Gain control by sparse, ultra-slow glycinergic synapses. *Cell Rep.* 38:110410. <https://doi.org/10.1016/j.celrep.2022.110410>

Jensen, R.J. 2006. Activation of group II metabotropic glutamate receptors reduces directional selectivity in retinal ganglion cells. *Brain Res.* 1122: 86–92. <https://doi.org/10.1016/j.brainres.2006.08.119>

Kaneda, M., K. Ishii, Y. Morishima, T. Akagi, Y. Yamazaki, S. Nakanishi, and T. Hashikawa. 2004. OFF-cholinergic-pathway-selective localization of P2X2 purinoceptors in the mouse retina. *J. Comp. Neurol.* 476:103–111. <https://doi.org/10.1002/cne.20208>

Kaneda, M., K. Ito, Y. Morishima, Y. Shigematsu, and Y. Shimoda. 2007. Characterization of voltage-gated ionic channels in cholinergic amacrine cells in the mouse retina. *J. Neurophysiol.* 97:4225–4234. <https://doi.org/10.1152/jn.01022.2006>

Kaneda, M., M. Hashimoto, and A. Kaneko. 1995. Neuronal nicotinic acetylcholine receptors of ganglion cells in the cat retina. *Jpn. J. Physiol.* 45: 491–508. <https://doi.org/10.2170/jjphysiol.45.491>

Kaneda, M., T. Ishii, and T. Hosoya. 2008. Pathway-dependent modulation by P2-purinoceptors in the mouse retina. *Eur. J. Neurosci.* 28:128–136. <https://doi.org/10.1111/j.1460-9568.2008.06317.x>

Kittila, C.A., and S.C. Massey. 1997. Pharmacology of directionally selective ganglion cells in the rabbit retina. *J. Neurophysiol.* 77:675–689. <https://doi.org/10.1152/jn.1997.77.2.675>

Koren, D., J.C.R. Grove, and W. Wei. 2017. Cross-compartmental modulation of dendritic signals for retinal direction selectivity. *Neuron.* 95: 914–927.e4. <https://doi.org/10.1016/j.neuron.2017.07.020>

Lee, S., K. Kim, and Z.J. Zhou. 2010. Role of ACh-GABA cotransmission in detecting image motion and motion direction. *Neuron.* 68:1159–1172. <https://doi.org/10.1016/j.neuron.2010.11.031>

Lin, B., and R.H. Masland. 2006. Populations of wide-field amacrine cells in the mouse retina. *J. Comp. Neurol.* 499:797–809. <https://doi.org/10.1002/cne.21126>

Lipton, S.A., E. Aizenman, and R.H. Loring. 1987. Neural nicotinic acetylcholine responses in solitary mammalian retinal ganglion cells. *Pflugers Arch.* 410:37–43. <https://doi.org/10.1007/BF00581893>

Majumdar, S., J. Weiss, and H. Wässle. 2009. Glycinergic input of widefield, displaced amacrine cells of the mouse retina. *J. Physiol.* 587:3831–3849. <https://doi.org/10.1113/jphysiol.2009.171207>

Masland, R.H., and J.W. Mills. 1979. Autoradiographic identification of acetylcholine in the rabbit retina. *J. Cell Biol.* 83:159–178. <https://doi.org/10.1083/jcb.83.1.159>

Masland, R.H., J.W. Mills, and S.A. Hayden. 1984. Acetylcholine-synthesizing amacrine cells: Identification and selective staining by using radioautography and fluorescent markers. *Proc. R. Soc. Lond. B.* 223:79–100. <https://doi.org/10.1098/rspb.1984.0084>

Matsumoto, A., W. Agbariah, S.S. Nolte, R. Andrawos, H. Levi, S. Sabbah, and K. Yonehara. 2021. Direction selectivity in retinal bipolar cell axon terminals. *Neuron.* 109:2928–2942.e8. <https://doi.org/10.1016/j.neuron.2021.07.008>

Menger, N., D.V. Pow, and H. Wässle. 1998. Glycinergic amacrine cells of the rat retina. *J. Comp. Neurol.* 401:34–46. [https://doi.org/10.1002/\(SICI\)1096-9861\(19981109\)401:1<34::AID-CNE3>3.0.CO;2-P](https://doi.org/10.1002/(SICI)1096-9861(19981109)401:1<34::AID-CNE3>3.0.CO;2-P)

Myhr, K.L., and J.S. McReynolds. 1996. Cholinergic modulation of dopamine release and horizontal cell coupling in mudpuppy retina. *Vis. Res.* 36: 3933–3938. [https://doi.org/10.1016/S0042-6989\(96\)00131-9](https://doi.org/10.1016/S0042-6989(96)00131-9)

Neal, M.J., J.R. Cunningham, and K.L. Matthews. 2001. Activation of nicotinic receptors on GABAergic amacrine cells in the rabbit retina indirectly stimulates dopamine release. *Vis. Neurosci.* 18:55–64. <https://doi.org/10.1017/S0952523801181058>

Nelson, R., E.V. Famiglietti Jr., and H. Kolb. 1978. Intracellular staining reveals different levels of stratification for on- and off-center ganglion cells in cat retina. *J. Neurophysiol.* 41:472–483. <https://doi.org/10.1152/jn.1978.41.2.472>

Ozaita, A., J. Petit-Jacques, B. Völgyi, C.S. Ho, R.H. Joho, S.A. Bloomfield, and B. Rudy. 2004. A unique role for Kv3 voltage-gated potassium channels in starburst amacrine cell signaling in mouse retina. *J. Neurosci.* 24: 7335–7343. <https://doi.org/10.1523/JNEUROSCI.1275-04.2004>

Pang, J.-J., F. Gao, and S.M. Wu. 2012. Physiological characterization and functional heterogeneity of narrow-field mammalian amacrine cells. *J. Physiol.* 590:223–234. <https://doi.org/10.1113/jphysiol.2011.222141>

Park, S.J.H., I.-J. Kim, L.L. Looger, J.B. Demb, and B.G. Borghuis. 2014. Excitatory synaptic inputs to mouse on-off direction-selective retinal ganglion cells lack direction tuning. *J. Neurosci.* 34:3976–3981. <https://doi.org/10.1523/JNEUROSCI.5017-13.2014>

Pei, Z., Q. Chen, D. Koren, B. Gianninaro, H. Acaron Ledesma, and W. Wei. 2015. Conditional knock-out of vesicular GABA transporter gene from starburst amacrine cells reveals the contributions of multiple synaptic mechanisms underlying direction selectivity in the retina. *J. Neurosci.* 35:13219–13232. <https://doi.org/10.1523/JNEUROSCI.0933-15.2015>

Peng, Y.R., R.E. James, W. Yan, J.N. Kay, A.L. Kolodkin, and J.R. Sanes. 2020. Binary fate choice between closely related interneuronal types is determined by a Fezf1-dependent postmitotic transcriptional switch. *Neuron.* 105:464–474.e6. <https://doi.org/10.1016/j.neuron.2019.11.002>

Pérez De Sevilla Müller, L., J. Shelley, and R. Weiler. 2007. Displaced amacrine cells of the mouse retina. *J. Comp. Neurol.* 505:177–189. <https://doi.org/10.1002/cne.21487>

Petit-Jacques, J., B. Völgyi, B. Rudy, and S. Bloomfield. 2005. Spontaneous oscillatory activity of starburst amacrine cells in the mouse retina. *J. Neurophysiol.* 94:1770–1780. <https://doi.org/10.1152/jn.00279.2005>

Reed, B.T., F.R. Amthor, and K.T. Keyser. 2002. Rabbit retinal ganglion cell responses mediated by alpha-bungarotoxin-sensitive nicotinic acetylcholine receptors. *Vis. Neurosci.* 19:427–438. <https://doi.org/10.1017/S0952523802194053>

Reed, B.T., K.T. Keyser, and F.R. Amthor. 2004. MLA-sensitive cholinergic receptors involved in the detection of complex moving stimuli in retina. *Vis. Neurosci.* 21:861–872. <https://doi.org/10.1017/S0952523804216066>

Sabbah, S., D. Berg, C. Papendorp, K.L. Briggman, and D.M. Berson. 2017. A cre mouse line for probing irradiance- and direction-encoding retinal networks. *eNeuro.* 4:1–21. <https://doi.org/10.1523/ENEURO.0065-17.2017>

Schmidt, M., M.F. Humphrey, and H. Wässle. 1987. Action and localization of acetylcholine in the cat retina. *J. Neurophysiol.* 58:997–1015. <https://doi.org/10.1152/jn.1987.58.5.997>

Schmidt, M., H. Wässle, and M. Humphrey. 1985. Number and distribution of putative cholinergic neurons in the cat retina. *Neurosci. Lett.* 59: 235–240. [https://doi.org/10.1016/0304-3940\(85\)90137-5](https://doi.org/10.1016/0304-3940(85)90137-5)

Sethuramanujam, S., A.J. McLaughlin, G. deRosenroll, A. Hoggard, D.J. Schwab, and G.B. Awatramani. 2016. A central role for mixed acetylcholine/GABA transmission in direction coding in the retina. *Neuron.* 90:1243–1256. <https://doi.org/10.1016/j.neuron.2016.04.041>

Sethuramanujam, S., G.B. Awatramani, and M.M. Slaughter. 2018. Cholinergic excitation complements glutamate in coding visual information in retinal ganglion cells. *J. Physiol.* 596:3709–3724. <https://doi.org/10.1113/JPhysiol.2017.212503>

Straschill, M., and J. Perwein. 1973. The effect of iontophoretically applied acetylcholine upon the cat's retinal ganglion cells. *Pflugers Arch.* 339: 289–298. <https://doi.org/10.1007/BF00594164>

Tauchi, M., and R.H. Masland. 1984. The shape and arrangement of the cholinergic neurons in the rabbit retina. *Proc. R. Soc. Lond. B.* 223: 101–119. <https://doi.org/10.1098/rspb.1984.0085>

Taylor, W.R., S. He, W.R. Levick, and D.I. Vaney. 2000. Dendritic computation of direction selectivity by retinal ganglion cells. *Science.* 289: 2347–2350. <https://doi.org/10.1126/science.289.5488.2347>

Taylor, W.R., and R.G. Smith. 2012. The role of starburst amacrine cells in visual signal processing. *Vis. Neurosci.* 29:73–81. <https://doi.org/10.1017/S0952523811000393>

Taylor, W.R., and D.I. Vaney. 2002. Diverse synaptic mechanisms generate direction selectivity in the rabbit retina. *J. Neurosci.* 22:7712–7720. <https://doi.org/10.1523/JNEUROSCI.22-17-07712.2002>

Taylor, W.R., and H. Wässle. 1995. Receptive field properties of starburst cholinergic amacrine cells in the rabbit retina. *Eur. J. Neurosci.* 7: 2308–2321. <https://doi.org/10.1111/j.1460-9568.1995.tb00652.x>

Vlasits, A.L., R. Bos, R.D. Morrie, C. Fortuny, J.G. Flannery, M.B. Feller, and M. Rivlin-Etzion. 2014. Visual stimulation switches the polarity of excitatory input to starburst amacrine cells. *Neuron.* 83:1172–1184. <https://doi.org/10.1016/j.neuron.2014.07.037>

Voigt, T. 1986. Cholinergic amacrine cells in the rat retina. *J. Comp. Neurol.* 248:19–35. <https://doi.org/10.1002/cne.902480103>

Völgyi, B., D. Xin, Y. Amarillo, and S.A. Bloomfield. 2001. Morphology and physiology of the polyaxonal amacrine cells in the rabbit retina. *J. Comp. Neurol.* 440:109–125. <https://doi.org/10.1002/cne.1373>

Watanabe, D., H. Inokawa, K. Hashimoto, N. Suzuki, M. Kano, R. Shigemoto, T. Hirano, K. Toyama, S. Kaneko, M. Yokoi, et al. 1998. Ablation of cerebellar Golgi cells disrupts synaptic integration involving GABA

inhibition and NMDA receptor activation in motor coordination. *Cell*. 95:17–27. [https://doi.org/10.1016/S0092-8674\(00\)81779-1](https://doi.org/10.1016/S0092-8674(00)81779-1)

Wei, W., A.M. Hamby, K. Zhou, and M.B. Feller. 2011. Development of asymmetric inhibition underlying direction selectivity in the retina. *Nature*. 469:402–406. <https://doi.org/10.1038/nature09600>

Yan, W., M.A. Laboulaye, N.M. Tran, I.E. Whitney, I. Benhar, and J.R. Sanes. 2020. Mouse retinal cell atlas: Molecular identification of over sixty amacrine cell types. *J. Neurosci.* 40:5177–5195. <https://doi.org/10.1523/JNEUROSCI.0471-20.2020>

Yazejian, B., and G.L. Fain. 1993. Whole-cell currents activated at nicotinic acetylcholine receptors on ganglion cells isolated from goldfish retina. *Vis. Neurosci.* 10:353–361. <https://doi.org/10.1017/S0952523800003746>

Yoshida, K., D. Watanabe, H. Ishikane, M. Tachibana, I. Pastan, and S. Nakanishi. 2001. A key role of starburst amacrine cells in originating retinal directional selectivity and optokinetic eye movement. *Neuron*. 30:771–780. [https://doi.org/10.1016/S0896-6273\(01\)00316-6](https://doi.org/10.1016/S0896-6273(01)00316-6)

Zemon, V., J. Gordon, and J. Welch. 1988. Asymmetries in ON and OFF visual pathways of humans revealed using contrast-evoked cortical potentials. *Vis. Neurosci.* 1:145–150. <https://doi.org/10.1017/S0952523800001085>

Zhang, C., and M.A. McCall. 2012. Receptor targets of amacrine cells. *Vis. Neurosci.* 29:11–29. <https://doi.org/10.1017/S0952523812000028>

Zheng, J.J., S. Lee, and Z.J. Zhou. 2004. A developmental switch in the excitability and function of the starburst network in the mammalian retina. *Neuron*. 44:851–864. <https://doi.org/10.1016/j.neuron.2004.11.015>